Korean J. Chem. Eng., 35(1), 298-302 (2018)
DOI: 10.1007/s11814-017-0240-9

pISSN: 0256-1115
eISSN: 1975-7220

Enhancement of thermal stability and chemical reactivity of phenolic resin ameliorated by nanoSiO$_2$

Yajun Guo*, Lihong Hu*,†, Puyou Jia*, Baofang Zhang, and Yonghong Zhou***

*Institute of Chemical Industry of Forest Products, CAF, Nanjing 210042, China
**School of Packaging, Michigan State University, East Lansing, MI48824, U.S.A.
(*Received 5 July 2017 • accepted 27 August 2017*)

Abstract−Phenolic resin has unsatisfactory thermal stability owing to the poor anti-oxidation property of methylene and phenol groups. To overcome this defect, a series of phenolic resin modified by nanoSiO$_2$ based on the tetraethoxysilane (TEOS) was successfully prepared via sol-gel method using phenol as solvent. The effect of nanoSiO$_2$ on the structures and properties of phenolic resin/foam was investigated. TGA and DTG indicated that the initial decomposition temperature of PR-0.5 (TEOS accounted for 0.5% of phenolic resin) was 41.8 °C higher than the neat PR-0. DSC revealed that the peak temperature presented a parabolic shape with the dosage of the TEOS, its maximal value resting on the PR-0.5. FT-IR and XRD demonstrated that chemical crosslink was reacted between PR and nanoSiO$_2$ hydrolyzed by the TEOS, forming new chemical bands. Reactivity analysis illustrated that the free phenol content and the hydroxymethyl group content changed sharply in PF-0.5, implying it has highest reactivity.

Keywords: Sol-gel Method, Phenolic Resin, NanoSiO$_2$, Free Phenol, Hydroxymethyl Group

INTRODUCTION

Phenolic resin, epoxy resin and unsaturated polyester resin are considered as three primary thermosetting resins. Compared with the latter two, phenolic resin has very distinctive properties: excellent flame retardancy, high char yield during pyrolysis and perfect sound insulation effect. Nevertheless, the methylene and phenolic hydroxyl group located in phenolic resin are of poor antioxidation, resulting in the decrease of active group and limiting its extensive applications in other areas tremendously. Therefore, it is a hot point of how to enhance the thermal stability, but meantime, not damaging its chemical reactivity [1].

Many methods have been explored to improve the thermal stability of phenolic resin. Some researchers modified phenolic resin with graphene, being of a single-layered two dimensional structure, which has a pronounced influence on the thermal stability [2-4]. Many prepared the compound materials by means of phenolic resin as matrix and carbon fiber or glass fiber as reinforcement, improvement of thermal stability and mechanical strength simultaneously [5-7]. Moreover, others introduced inorganic components into phenolic resin such as boron [8-11], phosphorous [12-14], silicon [15-18], their existence resembling a nucleus, combining organic phase with inorganic phase closely.

Owing to their properties of surface effect, small size effect and macro quantum, nanoparticles have widespread applications in the chemical field, among which nanoSiO$_2$ is prominent. Roumeli et al. [19] and Lin et al. [20] synthesized a series of urea-formaldehyde/nanoSiO$_2$ resins, of which the thermal analysis indicated that their thermal stability was enhanced obviously. Li et al. [21] and Shi et al. [22] modified epoxy resin with different dosage of nanoSiO$_2$. The result analysis showed that optimal value of nanoSiO$_2$ introduction was 4 wt% due to its best performance in heat endurance. Gao et al. [23] prepared a series of polyurethane/SiO$_2$ nanocomposites via in situ polymerization. The studies revealed that compatibility and thermal property were more excellent compared to the pure one. In brief, nanoSiO$_2$ has extensive applications in terms of thermal behavior of various resins.

Li et al. [24] claimed that silicone phenolic resin was synthesized via esterification reaction between methyltrimethoxysilane and novolac phenolic resin. The research shows both thermal stability and oxidation resistance were improved. Li et al. [25] conveyed that a certain content of silica sol can enhance the mechanical properties of PF/Silica nanocomposites, and the optimal performance was confirmed when the silica content reached 2 wt%. Periadurai et al. [26] showed that the PF modified with 5 wt% fumed silica had better thermal stability and was more flame retardant than the pure one.

In our work, nanoSiO$_2$ solution was first prepared via sol-gel process using tetraethoxysilane (TEOS) as precursor and phenol as solvent. Then the phenolic resin/nanoSiO$_2$ composites (PRs) were synthesized by blending the mixture with formaldehyde under alkaline condition. Ultimately, phenolic foam/nanoSiO$_2$ composites (PFs) were prepared by uniformly mixing the PRs with a surfactant, a foaming agent, a curing agent. For the sake of exploring the chemical groups in the PRs, Fourier transform infrared spectroscopy (FTIR) test was conducted. X-ray diffraction (XRD) was designed to perform a thorough characterization inside the PFs. To evaluate the thermal stability of the PRs as temperature increases, weight loss was measured by using thermogravimetric analysis (TGA). Differential scanning calorimetry (DSC) was performed to

†To whom correspondence should be addressed.
E-mail: zhlh990907@sina.com

investigate the curing reaction behavior of phenolic foam.

EXPERIMENTAL

1. Materials

Phenol, was purchased from Nanjing Chemical Reagent Co., China. Formaldehyde (polymer grade), urea, sodium hydroxide, were obtained from Shanghai Titan Co., Ltd., China. TEOS, ammonia, Tween80, n-pentane, were supplied by Sinopharm Chemical Reagent Co. Ltd. China. H_2O_2 (30% solution) was provided from Shanghai Zhanyun Chemical Co. Ltd. China. Calcium lignosulfonate (technical grade), was donated by the Guangxi Academy of Science. Catalysts used for the reaction between phenol and Formaldehyde were the laboratory-made.

2. Preparation of nanoSiO$_2$ Solution via Sol-gel Method

NanoSiO$_2$ solution was synthesized in a 500 ml four-neck round-bottom flask reactor equipped with a stirrer, a thermometer, a constant-pressure separating funnel and a reflux condenser. Phenol (100 g, 1.05 mol), The amount of TEOS was 0.1%, 0.2%, 0.5%, 0.7%, 1% by weight of phenolic resin, were added into the flask, stirred and heated to 40 °C, respectively. Then the mixture including ammonia (0.409, 0.818, 2.045, 2.863, 4.090 g) and deionized water (0.511, 1.023, 2.556, 3.578, 5.110 g) in the constant-pressure separating funnel was added drop by drop in one hour. After 1 h reaction time, the blue nanoSiO$_2$ solution was obtained.

3. Synthesis of Pure PR and PRs

The PRs, designated as PR-0.1, PR-0.2, PR-0.5 PR-0.7 and PR-1 with respect of TEOS content, were prepared in a 1,000 ml three-neck round-bottom flask reactor equipped with a stirrer, a thermometer, and a reflux condenser. Phenol (100 g, 1.05 mol), and catalysts (6 g) were mixed into the flask when the temperature of water bath reached 70 °C. Then formaldehyde (96 g, 3.17 mol) was poured into the flask three times (25 g+35 g+36 g). The process had to be treated carefully to prevent a sharp rise in temperature. The blue nanoSiO$_2$ solution was poured into the reaction system at 70 °C. After 2 h reaction time at 85 °C, urea (24 g) was added to the resin to neutralize the excess formaldehyde. After cooling to 50 °C during a 0.5 h period of time, the PRs were prepared. The pure PR, that is PR-0, was prepared in accordance with the same process without TEOS.

4. Preparation of Neat PF and PFs

PR/PFs (80 g), Tween80 (1.6 g), and n-pentane (6 g) were mixed for 3 min, into the 200 ml plastic breaker under rapid stirring at 1,000 rpm. The curing agent (20 g, laboratory-made) was added, slowly stirring at 500 rpm for 2 min and rapid stirring at 2,000 rpm for 1 min. Then the mixture was poured into a mould (200 mm×200 mm×50 mm), which had been heated to 70 °C in the oven.

5. Measurements

FTIR measurements were performed on a Nicolet IS10 IR spectrometer (Nicolet Co., USA) with the wave number range of 400-4,000 cm^{-1}. TG analysis was on a TG209F1 (Netzsch Co., Germany) from room temperature to 800 °C at the heating rate of 20 °C/min in nitrogen atmosphere. DSC was on a DSC 204 calorimeter (Netzsch Co., Germany) under nitrogen atmosphere at the heating rate of 10 °C/min, placed in stainless steel closed aluminum crucibles with the temperature range from room temperature to 300 °C. XRD analysis was recorded on the D8 Focus X-ray diffractometer (Bruker AXS Co., Germany) at 40 kV and 30 mA, a step size of 0.04° and a step time of 0.1 s, using Cu Kα radiation and 2θ range of 10-100°. The characteristics of free phenol and hydroxymethyl group content were determined according to the standards GB/T 14074-2006.

RESULTS AND DISCUSSION

1. Thermal Properties

It is common sense that the service cycle and application field of the material depend on its thermal stability. That is why it has been paid attention to by more and more researchers recently. TGA and DTG curves of the PR-0 and modified PRs are shown in Fig. 1. From the curves we can see they have similar decomposition characteristics, that is, represented as three-step stages: there appears first a sharp weight loss followed by a condition that mass reduction turns smooth. One explanation for this phenomenon can be the release of the redundant water, free aldehyde and phenol, low oligomer (first stage); the condensation reaction leading to the crosslink network structure (second stage), and the precipitation of organic compounds rooting in the reaction of the residual func-

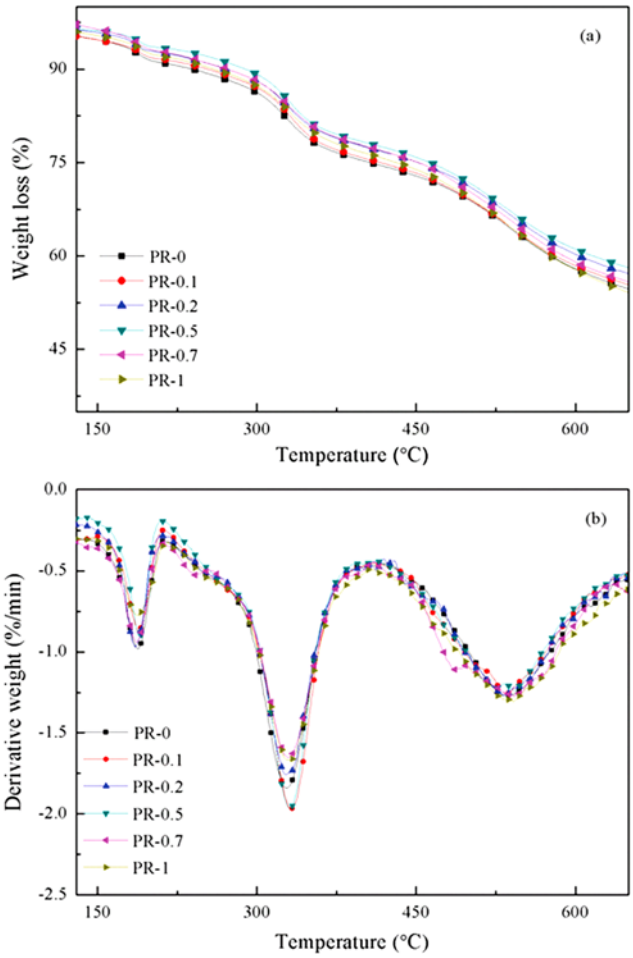

Fig. 1. The TGA (a) and DTG (b) curves of PR and PRs.

Table 1. The Td_5, Td_{20} and char residual of neat PR and PRs

Samples	Td_5 (°C)	Td_{20} (°C)	Char residual (%)
PR-0	141.3	340.2	49.68
PR-0.1	142.5	344.1	50.73
PR-0.2	173.8	359.5	52.45
PR-0.5	183.1	367.8	53.73
PR-0.7	179.1	362.2	50.95
PR-1	161.4	350.5	49.95

Td_5: the temperature of 5% mass loss
Td_{20}: the temperature of 20% mass loss

tional groups, respectively [27].

It is clear that the introduction of silica promotes the thermal stability of the copolymer. As Table 1 shows, for instance, Td_5, as defined by the temperature of 5% mass loss, are 141.3 °C and 183.1 °C of the PR-0 and PR-0.5. Furthermore, the temperature of 20% residual mass (Td_{20}) of the PR-0 and PR-0.5 are shifted by 340.2 to 367.8 °C, while the char residual of PR-0.5 than PR-0 improved by 49.68% to 53.73% at 796.9 °C. In short, the modified PRs shows improved thermal stability on the basis of the pure PR, among which the PR-0.5 is best. According to the published literature [28], this can be explained by the theory that newly generated carbonaceous silicate structure is attached to the surface of the compounds during combustion, keeping the exterior tinder from delivering and preventing the inner mass from being burned even further. However, it was established that agglomeration would happen in a bigger chance with excessive nanoSiO_2, which not only can not enhance the performance of polymer, but turns into new defect. That is why the indicators of the PR-1 are lower than the PR-0.5 slightly.

2. Curing Reaction Behavior

The effect of nanoSiO_2 on curing reactions of the resin was characterized by the DSC in the Fig. 2. The phenomenon is that they have a similar curve trend except from the maximum peak temperature approaching the high temperature region. With the increase of TEOS content, the peak temperature was fixed at 176.32 °C of

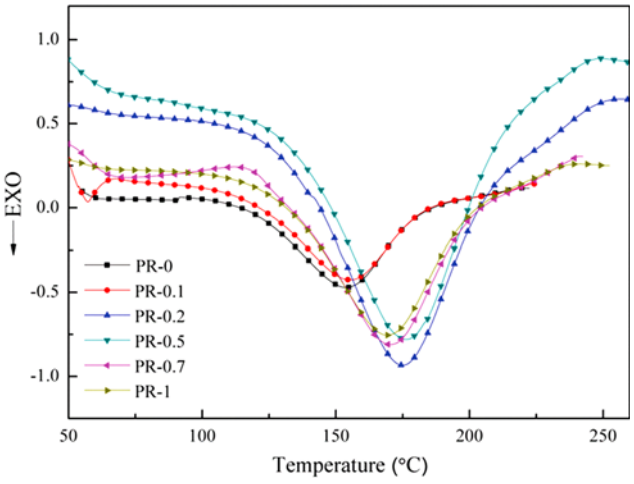

Fig. 2. The DSC curves of PR and PRs.

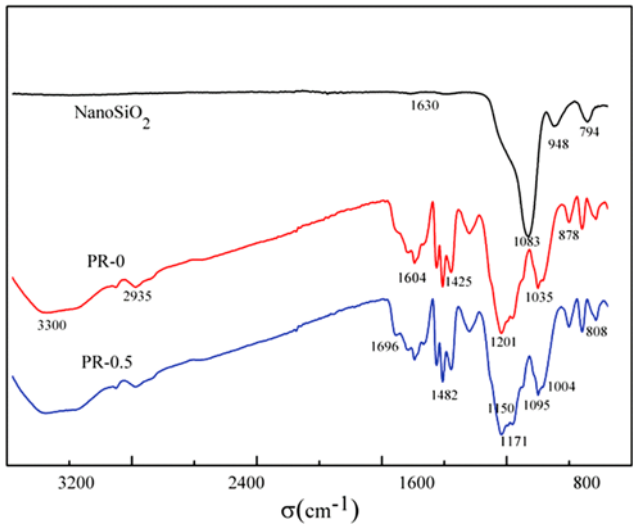

Fig. 3. The FTIR spectra of nanoSiO_2, PR-0 and PR-0.5.

the PR-0.5, higher than 154.03 °C on behalf of the PR-0, until it dropped to 169.60 °C related to PR-1. It may be explained that the introduction of nanoSiO_2 reacted with the resin matrix, forming a more compact cross-linked network structure and impeding the movement of polymer chains. Therefore, it needs more energy to overcome the interaction force between the matrix (phenolic resin) and the reinforcement (nanoSiO_2), which can be confirmed by using Kissinger¢s method [29]. However, the excessive agglomeration of nanoSiO_2 results in the available nanoSiO_2 turning fewer, which can do a condensation reaction with ph-OH or ph-CH_2OH, not impeding the curing reaction progress while the temperature corresponding to the curing peak is turning lower once again naturally.

3. Structure Characterization

Fig. 3 shows the FTIR spectra of nanoSiO_2, PR-0 and PR-0.5. First, for PR-0, the apparent absorption peaks located at 3,300 cm^{-1} and 2,935 cm^{-1} correspond to the phenolic hydroxyl and methylene, respectively. Meanwhile, other characteristic absorption bands lying in 1,604, 1,201, and 878 cm^{-1} are attributed to the C=C double bond asymmetric stretching, C-O stretching vibration, and -CH- flexural vibration, respectively. Compared to the neat PR, the PR-0.5 has two new absorption peaks at 1,095 and 808 cm^{-1} signifying the representative stretching vibration of Si-O-Si bond and Si-O, which can be found easily at the FTIR spectra of nano-SiO_2 at the same time [30]. Moreover, a peak at 1,035 cm^{-1} standing for hydroxymethyl absorption turns weak in PR-0.5 than PR-0. Hence, it is concluded that a chemical crosslink reaction came into being between PR and nanoSiO_2 particles.

4. Inner Regularity

X-ray diffraction analysis was conducted. Fig. 4 plots a comparison of the different patterns of the nanoSiO_2, PF-0 and PFs. For the XRD pattern of the nanoSiO_2, it is obvious that a broad diffraction peak appears at 22.8, which is a characteristic peak, indicating the formation of an amorphous phase. The foams, including pure and modified foam, present a relatively sharp peak around 20. Meantime, a slight left shift of the peak occurs from PF-0 to

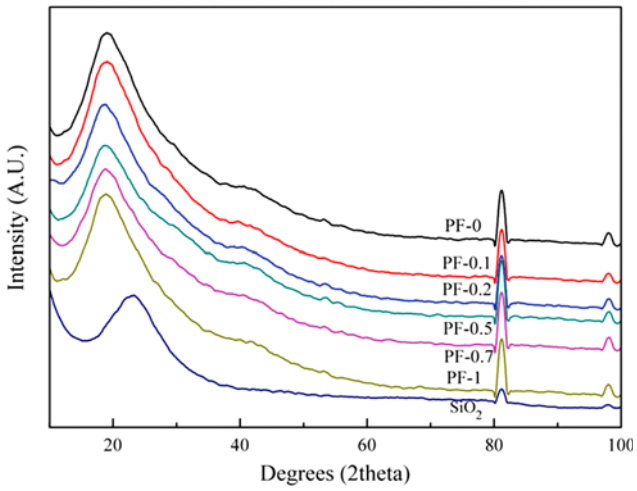

Fig. 4. The XRD patterns of nanoSiO$_2$, PF and PFs.

PF-0.5 successively (2θ=19.6, 19.1, 18.8, 18.5) and then maintains the value of PF-0.5, PF-0.7, PF-1, basically stabilized at a level of 18.5. The peak of modified foams seems to be sharper than pure foam, which may be attributed to orientation behavior taking place in the foam interior along with the more introduction of the nanoSiO$_2$, manifesting better stereoregularity and higher degree of crystallinity ultimately [31].

5. Phenolic Resin Chemical Reactivity Analysis

The two indexes, the content of free phenol and hydroxymethyl group, were used to describe the chemical reactivity of phenolic resin. The high reactivity of resin illustrates that substantial hydroxymethyl groups located in the ortho-para position of phenol were generated, which must consume massive phenol to participate in the addition reaction with formaldehyde, and therefore free phenol content turned low [32].

Fig. 5 shows the content variation of free phenol and hydroxymethyl group accompanied by the different addition of TEOS. One can conclude that the content of free phenol decreased, whereas that of hydroxymethyl group increased. This is probably attributed to the condensation reaction between hydroxyl groups seated on

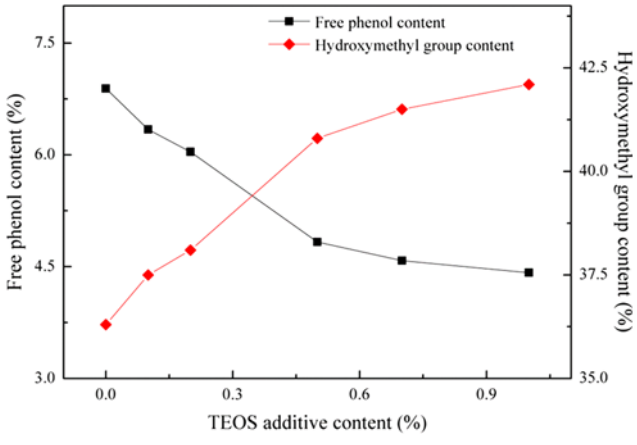

Fig. 5. The content variation of free phenol and hydroxymethyl group of PR and PRs.

the surface of nanoSiO$_2$ and phenolic hydroxyl or hydroxymethyl group, which consumption causes the reaction to move in a positive direction, decreasing the free phenol percentage. Meantime, the hydroxymethyl group cannot be excessively exhausted since not all the nanoSiO$_2$ was involved in the condensation reaction considering its auto polymerization. Generally speaking, the content of hydroxymethyl group can still maintain a relatively high value. Moreover, the slope of two curves is the most steep in PR-0.5, then it goes into moderate.

CONCLUSION

A series of phenolic resin modified by nanoSiO$_2$ based on the TEOS was successfully prepared via sol-gel method using phenol as solvent. TGA and DTG indicated that the PR-0.5 had excellent thermal stability compared to the neat PR-0. DSC revealed that the peak temperature presented a parabolic shape with the dosage of the TEOS, its maximal value resting on the PR-0.5. FT-IR and XRD demonstrated that chemical crosslink reaction came into being between PR and nanoSiO$_2$, forming the bond of Si-O-Si bond and Si-O. Reactivity analysis illustrated that the free phenol content decreased sharply until smoothed gradually and the hydroxymethyl group content increased swiftly to a high value. There was one thing in common that the extent of changes had the maximum value appear in PR-0.5. Hence, the PR-0.5/PF-0.5 had the optimal performance among the PRs/PFs. However, the limitations of this work should not be neglected, including how to describe the cure kinetics equation of PRs and how to measure accurately the distribution of nanoSiO$_2$ particles in PFs. Although this research provides an effective way to enhance the thermal stability of phenolic resin, the properties of the phenolic foam have not yet been characterized in detail, for instance, fragility and mechanical properties. Therefore, various measurements of phenolic foam need to be taken in future research.

ACKNOWLEDGEMENT

This work was funded by the National Natural Science Foundation of China (31470613), the Innovation Project of Institute of Chemical Industry of Forest Products (LHSXKQ11) and National Key Research and Development Program of China (2017YFD0601000).

REFERENCES

1. X. Y. Li, Z. Z. Wang and L. X. Wu, *RSC Adv.*, **5**, 99907 (2015).
2. A. A. Balandin, S. Ghosh, W. Bao, I. Calizo, D. Teweldebrhan and F. Miao, *Nano Lett.*, **8**, 902 (2008).
3. Y. H. Zhao, Z. K. Wu and S. L. Bai, *Compos. Part A-Appl. S.*, **72**, 200 (2015).
4. L. Zhao, X. Sun, Z. Lei, J. Zhao, J. Wu and Q. Li, *Compos. Part B-Eng.*, **83**, 317 (2015).
5. H. Cheng, H. Xue, C. Hong and X. Zhang, *Compos. Sci. Technol.*, **140**, 63 (2017).
6. S. A. Song, S. C. Yong and S. S. Kim, *Compos. Sci. Technol.*, **103**, 85 (2014).
7. Y. H. Zhao, Y. F. Zhang, S. L. Bai and X. W. Yuan, *Compos. Part B-*

Eng., **94**, 102 (2016).
8. S. Li, F. Chen, B. Zhang, Z. Luo, H. Li and T. Zhao, *Polym. Degrad. Stab*., **133**, 321 (2016).
9. H. Li, D. Yao, Q. Fu, L. Liu, Y. Zhang and X. Yao, *Carbon*, **52**, 418 (2013).
10. L. Kobera, J. Czernek, M. Strečková, M. Urbanova, S. Abbrent and J. Brus, *Macromolecules*, **48**, 4874 (2015).
11. C. T. Lin, H. T. Lee and J. K. Chen, *Appl. Surf. Sci*., **330**, 1 (2015).
12. S. Wang, X. Jing, Y. Wang and J. Si, *Polym. Degrad. Stab*., **99**, 1 (2014).
13. J. Feng, L. Chen, J. Gu, Z. He, J. Yun and X. Wang, *J. Polym. Res*., **23**, 1 (2016).
14. X. Sui and Z. Wang, *Polym. Adv. Technol*., **24**, 593 (2013).
15. G. Zhang, M. Shi, C. Huang and Z. Huang, *J. Macromol. Sci. B*., **55**, 810 (2016).
16. C. Li, J. Wan, Y. T. Pan, P. C. Zhao, H. Fan and D. Y. Wang, *ACS Sustain. Chem. Eng*., **4**, 3113 (2016).
17. J. Brus, M. Špírková, A. Drahomíra Hlavatá and A. Strachota, *Macromolecules*, **37**, 1346 (2004).
18. M. R. Schütz, K. Sattler, S. Deeken, O. Klein, V. Adasch and C. H. Liebscher, *J. Appl. Polym. Sci*., **117**, 2272 (2010).
19. E. Roumeli, E. Papadopoulou, E. Pavlidou, G. Vourlias, D. Bikiaris and K. M. Paraskevopoulos, *Thermochim. Acta*, **527**, 33 (2012).
20. Q. Lin, G. Yang, J. Liu and J. Rao, *Frontiers of Forestry in China*, **1**, 230 (2006).
21. H. Li, Z. Zhang and X, Ma, *Surf. Coat. Technol*., **201**, 5269 (2007).
22. H. Shi, F. Liu, L. Yang and E. Han, *Prog. Org. Coat*., **62**, 359 (2008).
23. X. Gao, Y. Zhu, X. Zhao, Z. Wang, D. An and Y. Ma, *Appl. Surf. Sci*., **257**, 4719 (2011).
24. S. Li, Y. Han, F. Chen, Z. Luo, H. Li and T. Zhao, *Polym. Degrad. Stab*., **124**, 68 (2016).
25. Q. Li, L. Chen, J. Zhang, K. Zheng, X. Zhang and F. Fang, *Polym. Eng. Sci*., **55**, 2783 (2016).
26. T. Periadurai, C. T. Vijayakumar and M. Balasubramanian, *J. Anal. Appl. Pyrol*., **89**, 244 (2010).
27. J. Yuan, Y. Zhang and Z. Wang, *J. Appl. Polym. Sci*., **132**, 42590 (2015).
28. I. M. Arafa, M. M. Fares and A. S. Barham, *Eur. Polym. J*., **40**, 1477 (2004).
29. H. E. Kissinger, *Anal. Chem*., **29**, 1702 (1957).
30. S. Li, F. Chen, Y. Han, H. Zhou, H. Li and T. Zhao, *Mater. Chem. Phys*., **165**, 25 (2015).
31. M. Su, Z. Wang, H. Guo, X. Li, S. Huang and L. Gan, *Adv. Powder Technol*., **24**, 921 (2013).
32. Y. F. Ma, J. F. Wang, Y. Z. Xu, C. P. Wang and F. X. Chu, *J. Therm. Anal. Calorim*., **114**, 1143 (2013).